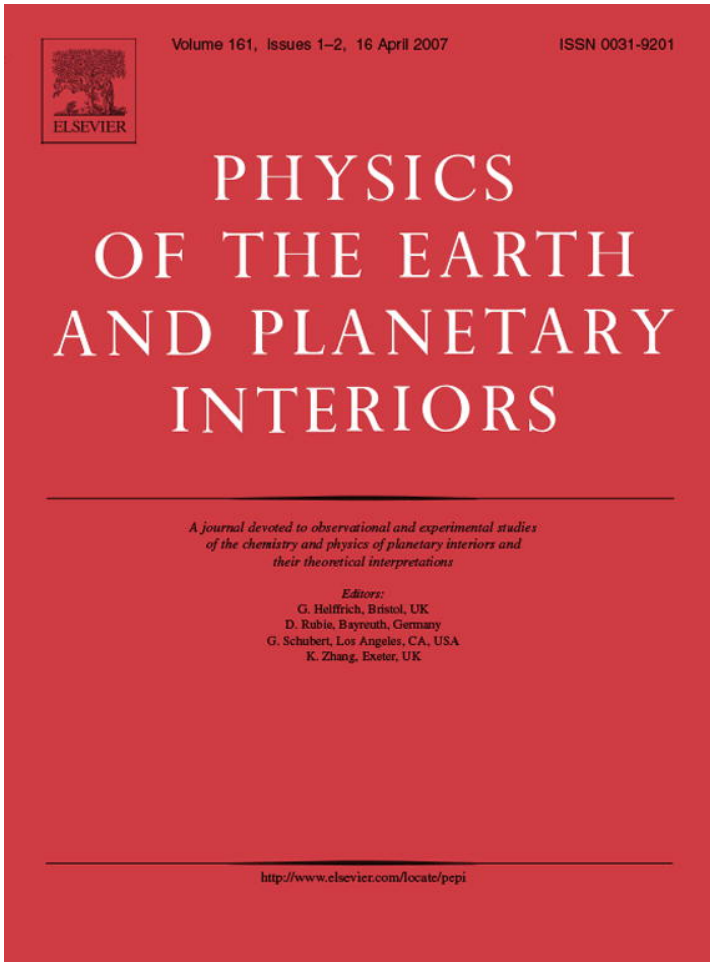

Available online at www.sciencedirect.com
ScienceDirect
Physics of the Earth and Planetary Interiors 161 (2007) 126–133
PHYSICS OF THE EARTH AND PLANETARY INTERIORS
www.elsevier.com/locate/pepi

Short communication

Laboratory derived constraints on electrical conductivity beneath Slave craton

Nikolai S. Bagdassarov [a,*], Maya G. Kopylova [b], Sandrine Eichert [c]

[a] *Institut für Geowissenschaften, Universität Frankfurt, Feldbergstraße 47, am Main D-60323, Germany*
[b] *Department of Earth and Ocean Sciences, The University of British Columbia, Vancouver, BC V6T 1Z4, Canada*
[c] *École et Observatoire des Sciences de la Terre, Université Louis Pasteur, 5 rue René Descart, Strasbourg Cedex F-67084, France*

Received 23 December 2005; received in revised form 5 January 2007; accepted 9 January 2007

Abstract

The depth profile of the electrical conductivity, $\sigma(d)$, beneath the Central Slave craton (Canada) has been reconstructed with the help of laboratory measurements carried out on peridotite xenoliths. $\sigma(T)$ of xenoliths was determined in the piston-cylinder apparatus at 1 and 2 GPa and from 600 to 1150 °C. $\sigma(T)$ of xenoliths follows the Arrhenius dependence with the activation energy, E_a, varying from 2.10 to 1.44 eV depending on temperature range and the Mg-number. The calculated xenolith geotherm and the suggested lithology beneath the Central Slave have been used to constrain $\sigma(d)$ as follows: $\sigma(d)$ in the crust varies between 0.5×10^{-5} and 10^{-3} S/m; the lithospheric $\sigma(d)$ sharply decreases below the Moho at 39.4 km to 0.5×10^{-8} S/m, which corresponds to 460 °C, and then gradually increases with the depth d to 0.5×10^{-2} S/m. The modeled MT-response of the constrained $\sigma(d)$ profile has been compared with MT-observations [Jones, A.G., Lezaeta, P., Ferguson, I.J., Chave, A.D., Evans, R.L., Garcia, X., Spratt J., 2003. The electrical structure of the Slave craton. Lithos, 71, 505–527]. The general trend of the calculated MT-response based on the $\sigma(d)$ model mimics the MT-inversion of the field data from the Central Slave.

PACS: 91.60.Pn; 93.30.Jg; 91.25.Qi; 91.35.Cb

Keywords: Craton; Xenoliths; Electrical conductivity; Magneto-telluric response

1. Background

Evolution of the thermal and mechanical thickness of the ancient lithosphere beneath stable cratons and continental platforms is still a puzzle for petrologists and geophysicists (Artemieva and Mooney, 2001; Sleep, 2003, 2005). The effective thickness of a chemically depleted layer, thermal and rheological boundary layers beneath Archean cratons, varies from 130 to 220 km according to geothermobarometry of xenoliths, from 150 to 250 km according to heat flow studies, and from 250 to 400 km according to teleseismic and reflected wave data (see review of Artemieva and Mooney, 2001). The general consensus exists on the fact that the thermal thickness of the Archean buoyant continental lithosphere has been stabilized soon after its formation and remains more or less constant since then, ~225 km (Sleep, 2003). The ancient cratonic lithosphere could be thermally eroded later, during continental accretion processes and its modern thickness could be thinner than the initial

* Corresponding author. Tel.: +49 6979840126; fax: +49 6979823280.
E-mail addresses: nickbagd@geophysik.uni-frankfurt.de (N.S. Bagdassarov), mkopylov@nexus.eos.ubc.ca (M.G. Kopylova), sandrine.eichert@cario.fr (S. Eichert).

0031-9201/$ – see front matter © 2007 Elsevier B.V. All rights reserved.
doi:10.1016/j.pepi.2007.01.001

one. The rate of the thermal erosion depends on the lateral size of the initial Archean continental block. The positive correlation between craton size and keel thickness indicates that the reworking of Archean lithosphere includes lithospheric erosion and chemical modifications of rocks and their properties in the whole lithospheric column. Ancient cratons that are smaller in size at the present time, experienced the largest thinning and reworking (Artemieva and Mooney, 2002). According to some electromagnetic surveys, the thickness of the ancient lithosphere, associated with a steep increase of $\sigma(d)$ as a function of depth d, is about 150–230 km (e.g. Schultz et al., 1993). However, these data are very difficult to interpret as a real lithospheric thickness because the electrical conductivity $\sigma(d)$ and seismic velocities vary not only with the depth d but also with the age or the timing of the continental accretion. In Archean, the mantle composition in general has been more chondritic than later. Thus, the reduced oxygen fugacity at that time has possibly influenced the Fe–Mg-mineralogical composition of the upper mantle rocks, which in turn resulted in a distinct contrast of the electrical conductivity profiles beneath ancient Archean cratons and later Proterozoic continents (Boerner et al., 1999).

In this paper, we have examined the electrical conductivity of peridotite xenoliths in laboratory and have constrained the electric conductivity profile, $\sigma(d)$ beneath Slave craton by using $\sigma(T)$ of xenoliths from the Central Slave. The xenolith geotherm calculated from the geothermobarometry of peridotite xenoliths of the Central Slave craton (Canada) has been used to estimate the depth profile of $\sigma(d)$.

2. Description of the Slave craton

The Slave craton in the N–W part of Canada is a small (about 600 km in N–S by 400 km in E–W) stable Archean craton hosting the oldest rocks ca. 4.03 Ga (Davis et al., 2003). Electro-magnetic studies (EM) demonstrated, that the Central Slave mantle contains a layer of the anomalously conductive rocks with a resistivity $< 20\,\Omega$ m at depths 80–130 km which coincides spatially with the ultradepleted layer of harzburgites (Jones et al., 2001, 2003). The nature of the high σ layer has been attributed to the presence of carbon on grain-boundaries of minerals and/or of C as a graphite phase while the depth of this conductor is above the graphite-diamond stability field (Jones et al., 2003). The tectonic origin and the structure of the central Slave lithosphere may be related to stacking and to the subcretion of exotic slabs at ca. 2.63 Ga ago (Davis et al., 2003). The missing link between EM conductivity anomaly and chemical depletion of the mantle peridotites could be a redox state of rocks beneath the craton (McCammon and Kopylova, 2004). In this paper, the $\sigma(d)$ model beneath Central Slave is revisited by using the laboratory derived $\sigma(T)$ of xenoliths from this area.

The lithology below the Central Slave is shown in Fig. 1 (left panel). The lower crustal mafic rocks ascribed to the Moho depth are likely to be granulitic (Pearson et al., 1999). The Moho boundary occurs at 39.4 km according to the teleseismic data (Bank et al., 2000) and does not correspond to a sharp change in the lithology. The change in the lithology from crustal to mantle rocks occurs somewhere within ca. 20 km, i.e. the crust-upper mantle boundary is grading from a mixture of felsic and mafic granulites for 10 km above the seismic Moho to a mixture of mafic granulites and mantle lherzolites for 10 km below the seismic Moho, with a decreasing proportion of mafic granulites upwards and downwards (Griffin and O'Reilly, 1987). The lower 10 km of the crust can be approximated by a mixture of granulites and rocks of the Central and the East Slave basement complexes, constituting the lower crust between 15 and 40 km in the Lac de Gras area (Bleeker, 2003). The shallow crust consists of the intermediate volcanic and trondjemite–tonalite–granite plutons (13–15 km); turbiditic greywackes (4–13 km), combined in one layer in Fig. 1, and granites (0–4 km). The upper 10 km of the mantle suggested to be composed of a mixture of granulites and spinel peridotites. The Central Slave mantle lithology is characterized by a shallow ultradepleted layer with a high ratio of low-Ca harzburgite to lherzolite extending down to ~150 km (Griffin et al., 1999). The deepest ultradepleted harzburgites are at 1100 ° C and $P = 5.3$ GPa or 159 km (Menzies et al., 2004). The transition from ultradepleted harzburgites to deeper lherzolites occurs from ~ 140 to ~160 km. Due to the similarity between the thermal state of the central and the N Slave lithospheres (Kopylova and Garo, 2004), the depth facies of peridotites in two locations should coincide. The ultradepleted low-Ca harzburgitic layer of the Central Slave continues to the North (Griffin et al., 1999; Kopylova and Garo, 2004). The overall thickness of the lithosphere beneath the Lac de Gras is bigger than near the S and SW margins. The lithosphere there consists of material like the deeper layer beneath Lac de Gras. The sharp boundary between the two layers suggests two different overlapping processes of the lithospheric evolution. The upper layer formed before and during the accretion stage of terrains (arcs, accreting edges) to the ancient continent. The deeper layer formed due to the ascending mantle plume (Griffin et al., 1999). The thermal interaction of the plume head with the ultradepleted

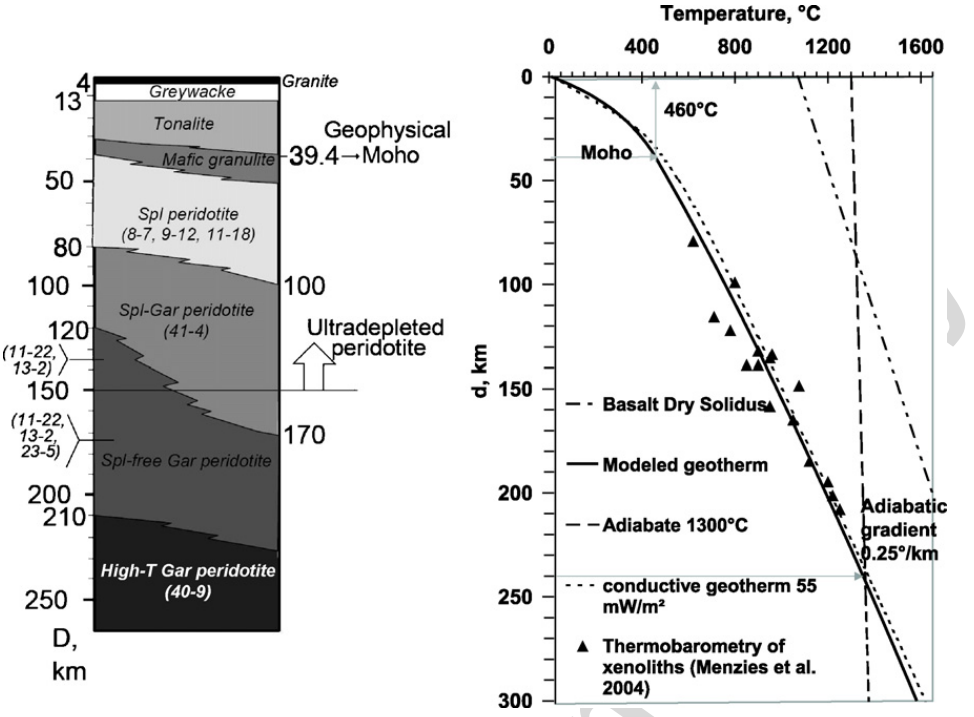

Fig. 1. Left panel: Central Slave lithology. Nomenclature of rocks and sample labels (numbers in parenthesis) are from Kopylova et al. (1999), Kopylova and Garo (2004) and McCammon and Kopylova (2004). Right panel: modeled $T(d)$ under the Central Slave craton. Thick line is the modeled geotherm, dotted line is the continental conductive geotherm with a surface heat flux $Q_0 = 55\,\mathrm{mW/m^2}$ and the intensity of the radiogenic heat production in the crust is $A = 2.16 \times 10^{-6}\,\exp(-d/20.7)$ in $\mathrm{W\,m^{-3}}$, where d is the depth in km. Triangles are PT-estimation of xenoliths from Menzies et al. (2004) according to the thermobarometry of Brey and Köhler (1990).

layer might have changed the electrical properties of deep rocks in central part of the Slave craton and might have caused an occurrence of the central Slave conductor. The minimum temperatures of 1150 ° C for high-T sheared peridotites (Pearson et al., 1999) indicate that the transition from low-T to high-T peridotite below central Slave begins at ~210 km (Fig. 1).

The mantle geotherm is derived from the Brey–Köhler thermobarometry (BK) of the mantle xenoliths (Menzies et al., 2004). The geotherm $T(d)$ beneath Central Slave has been calculated as follows:

- The heat capacity is $C_p = 1.24\,\mathrm{J\,kg^{-1}\,K^{-1}}$. T on the surface has been fixed to 283 K, at $d = 300$ km the heat flux in $\mathrm{W/m^2}$ is $3.75 \times 10^{-3}\,K_\mathrm{T}$, where K_T is the thermal conductivity in $\mathrm{W\,m^{-1}\,K^{-1}}$ at a corresponding $T(d)$ in K. At $d > 240$ km $T(d)$ follows the adiabate with the potential $T = 1280$ ° C and the gradient 0.25 K/km (Sleep, 2003). From 0 to 39.4 km depth K_T varies with d (in km) as $K_\mathrm{T} = 2.22 + 1.5 \times 10^{-2} d$. The intensity of the radiogenic heat production in the crust is assumed to be $A = 2.16 \times 10^{-6}\,\exp(-d/20.7)$ in $\mathrm{W\,m^{-3}}$. The density ρ in the upper 15 km of the crust is $2.5 \times 10^3\,\mathrm{kg\,m^{-3}}$ and from 15 to 36 km is $2.7 \times 10^3\,\mathrm{kg\,m^{-3}}$, in the upper mantle ρ is $3.2 \times 10^3\,\mathrm{kg\,m^{-3}}$ (Kopylova et al., 1999). From 38 to 240 km, the thermal conductivity K_T varies with d as $K_\mathrm{T} = 3.2[1 + 2.85 \times 10^{-4}(T - 728)]$ (Russel et al., 2001). The intensity of the heat radiogenic sources in the upper mantle at d from 36 to 120 km is fixed to $10^{-8}\,\mathrm{W\,m^{-3}}$, and at $d > 120$ km is 0. The calculated $T(d)$ using the finite element code (FEMLAB) is shown in Fig. 1, right panel.

3. Measurements of $\sigma(T)$ on xenoliths

The peridotite samples used for the measurements of $\sigma(T)$ are listed in Table 1. They are derived from the Jericho kimberlite of the N-Slave craton and were previously characterized by Kopylova et al. (1999) and Kopylova and Garo (2004). All types of the Central Slave peridotites are also found in the N-Slave at Jericho. In order to construct a model of $\sigma(d)$, $\sigma(T)$ of each peridotite sample has been measured in the piston-cylinder apparatus at $P = 1$–2 GPa and at $600 < T < 1150$ °C, below melting point.

The estimation of dc σ consists of measuring the complex electrical impedance $Z(\omega) = Re[Z(\omega)] + i \cdot Im[Z(\omega)]$, where ω is the frequency. The scans of $Z(\omega)$ from 100 kHz to 10 mHz were registered at each T

Table 1
Fitting parameters of $\sigma(T)$ of peridotite xenoliths from Slave craton (Canada) from Eq. (1)[a]

Sample description	$\ln \sigma_0$ [b]	E_a (eV)
Depth: 39.4–100 km		
40-16[c]: Spl Pd	5.35	1.44 (1.33–1.54)
8-7: Spl Lhz	7.88	1.70 (1.66–1.92)
11-18: Spl Pd	12.72	2.12 (1.88–2.17)
9-12: Spl Hbgh	8.82	1.75 (1.56–1.82)
Depth: 90–160 km		
41-4: Spl Gar Pd	10.10	1.84 (1.80–1.92)
Depth: 120–210 km		
13-2: low-T Gar Pd	15.07	2.23 (1.77–2.36)
Depth: 190–200 km		
23-5: fertile high-T Gar Pd	6.20	1.48 (1.32–1.59)
Depth: > 210 km		
40-9: high-T Gar Pd	8.77	2.02 (1.44–2.1)

[a] Activation energy in parenthesis corresponds to the intervals $T < 850\,^\circ$ C and $T > 850\,^\circ$C, respectively.
[b] σ_0 is in S/m.
[c] Nomenclature of rocks and sample labels are from Kopylova et al. (1999), Kopylova and Garo (2004) and McCammon and Kopylova (2004).

and P and proceeded on Argand-plots, i.e. the dependence of $-Im[Z]$ versus $Re[Z]$. The high ω-part of a plot represents a semi-circle and corresponds to the bulk properties. Data processing consisted of fitting of $-Im[Z]$ versus $Re[Z]$ to two $R-C$ constant phase elements connected in parallel. The bulk resistance is taken as an active resistance R of the high ω semi-circle. The specific resistance ϱ has been calculated using the known geometric factor of electrodes G_f: $\varrho = R \times G_f$. The measuring cell, which was in a shape of a co-axial cylindrical capacitor with electrodes made of Mo-foil 0.05 mm in thickness, has a geometric factor $G_f = 5$–6 cm. The starting powder samples having a grain size ca. 20–100 μm, have been sintered over ca. 70 h at 1 GPa and ca. 1100 °C. The piston-cylinder cell consisting of CaF_2, graphite and boron nitride, has been described elsewhere (Maumus et al., 2005). A typical f_{O_2} in the cell at 1200–1300 ° C is between IW and FMQ buffers (Maumus et al., 2005). These reduced conditions correspond to f_{O_2} estimations beneath the Slave based on the Mössbauer study of xenoliths (McCammon and Kopylova, 2004). The final dc conductivity data of rocks have been taken from the 2-day heating–cooling cycle. The 3-day heating–cooling cycle does not differ from the second one.

$\sigma(T)$ of the peridotite samples is presented in Fig. 2. $\sigma(T)$ of peridotites varies for ca. 1.5 orders of magnitude depending on the mineralogical composition. At $T < 800\,^\circ$C, the most conductive is the fertile lherzolite 23-5 having a large proportion of Gar, ca. 12.5 vol.%

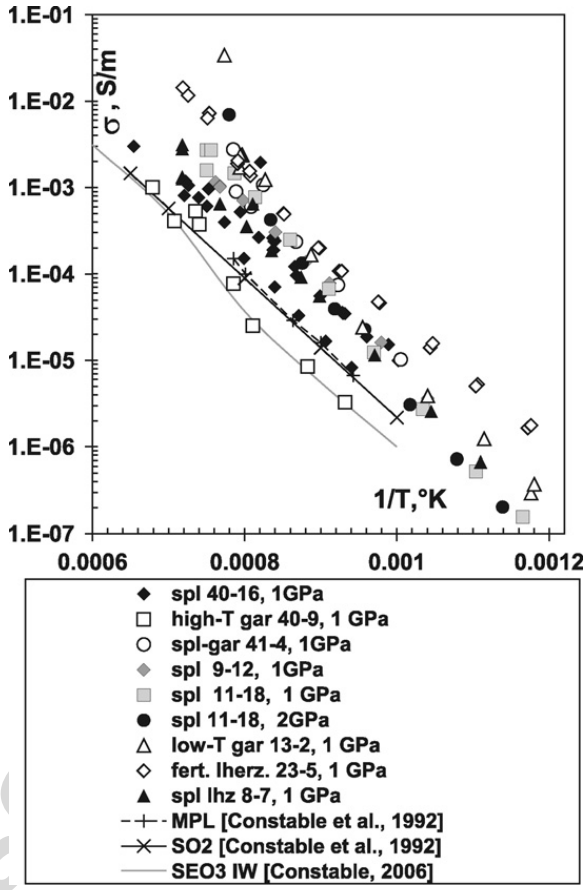

Fig. 2. Laboratory measurements of $\sigma(T)$ in peridotite xenoliths from Slave craton (Canada). MPL = Mt. Porndon garnet lherzolite (Constable et al., 1992), SO2 = standard olivine model (Constable et al., 1992), SEO3IW = a new standard electrical olivine model at IW-buffer (Constable, 2006).

(Kopylova and Russel, 2000), while at $T > 850\,^\circ$ C the most conductive is the low-T garnet lherzolite. The high-T garnet peridotite is less conductive at all temperatures and this rock corresponds to the deepest layer of the Central Slave lithosphere. σ of spinel peridotites which are all ultra-depleted, is similar to those of the garnet-bearing peridotites at a bigger depth. The average $\sigma(T)$ of all peridotites is close to the standard olivine model SO2 of Constable (1993) within ±0.5 lg units. At $T > 850\,^\circ$C, the activation energy of $\sigma(T)$ (E_a) for peridotites varies from 1.7 to 2.1 eV at 1 GPa. The electrical conductivity of the studied rocks is mainly controlled by σ of Ol, because E_a of Ol-crystals is 1.41 eV, while E_a of Px is ca. 1.8–1.9 eV (Tyburczy and Fisler, 1995). σ measured at 1 and 2 GPa does not show any significant pressure dependence of σ which is typical for olivine rich mafic rocks (Xu et al., 2000).

The depth model $\sigma(d)$ beneath the Central Slave craton is based on the Arrhenius equation

$$\ln(\sigma) = \ln \sigma_0 - \frac{E_a}{kT}, \quad (1)$$

where σ is the bulk electrical conductivity, σ_0 is the pre-exponential constant, E_a is the activation energy, k is the Boltzmann constant and T is the temperature in K. The constants, σ_0 and E_a for studied peridotites are listed in Table 1.

For modelling of $\sigma(d)$, a layer from 36 to 90 km has been taken as a mixture of spinel peridotites 11-18, 8-7 and 9-12 (Fig. 1). At $d > 90$ km, spinel-garnet peridotite 41-4 was added to the mixture, etc. $\sigma(T)$ has been calculated as an arithmetic mean value of $\log(\sigma_i(T))$ of individual rocks, i.e. according to a logarithmic mixing model of (Lichtenecker, 1926). Due to the closeness of maximum and minimum conductivities of peridotitic rocks the logarithmic mean values is about to Hashin–Shtrickman bounds, which have been calculated for rock mixing according to (Ledo and Jones, 2005).

The specific resistivity ϱ of the crust in Ω m has been approximated as follows:

- From 0 to 4 km: lg (ϱ) = 3.7–0.09 d, from 4 to 13 km: lg (ϱ) = 3.34 (Ingham, 1997).
- From 13 to 30 km: lg (ϱ) = 5.85–0.026 d + 3.47 × 10^{-4} d^2, which is the approximation of the data for quartz diorites from (Parkhomenko, 1967).
- From 30 to 39.4 km: lg (ϱ) = 11.9–0.19 d − 1.25 × 10^{-3} d^2, which represents an approximation of ϱ of a mixture consisting of quartz diorite and mafic granulite (Fuji-ta et al., 2004) with a continuous increase of the mafic granulite fraction from 0% at 30 km to 100% at 39.4 km. From 39.4 to 50 km, ϱ has been taken as a mixture of mafic granulite and peridotites with the continuous decreasing fraction of the mafic granulite from 100% at 39.4 km to 0% at 50 km depth. Below 50 km, $\varrho(T)$ has been calculated with the use of the constants of Eq. (1) from Table 1 and the lithology from Fig. 1. The left panel of Fig. 1 shows the smoothness of mineralogical boundaries. The conductivity between boundary layers has been calculated as a mixture of rocks which changes from 0% at a depth indicated on the left side to 100% at a depth indicated on the right side of the panel.

The modelled $\sigma(d)$ is shown in Fig. 3. In the crust, σ is from 2 × 10^{-6} to 10^{-3} S/m, sharply decreases below the Moho and then gradually increases with the depth. When the measured $\sigma(T)$ of spinel peridotites is interpolated to the Moho depth 39.4 km and T = 460 °C, the conductivity σ would be ∼10^{-7} S/m. This is a lower

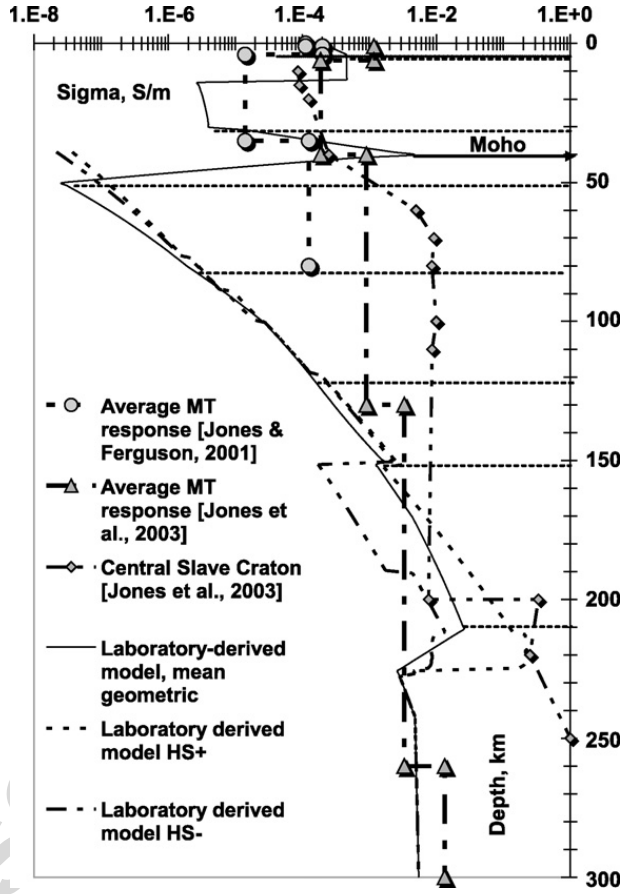

Fig. 3. Modeled σ profiles under Slave craton derived from laboratory experiments on peridotite xenoliths. $\sigma(d)$ obtained from the inversion of average MT-data (Jones and Ferguson, 2001; Jones et al., 2003) and the station Lac de Gras (Central Slave craton) are shown for comparison. $\sigma(d)$ for the upper and lower crust rocks are compiled σ for greywackes, tonalites and mafic granulites from Ingham (1997), Parkhomenko (1967) and Fuji-ta et al. (2004). HS upper and lower bounds were estimated from a mixture model of electrical conductivity from Ledo and Jones (2005).

limit to σ of the sub-Moho peridotite, as it is based on the extrapolation of σ measured at $T > 580$ ° C to lower T. In reality, the slope of $\sigma(T)$ is gentler at $T < 580$ ° C due to the change of the conductivity mechanism in Ol (Sakamoto et al., 2002). The change of the slope on the Arrhenius plots of $\sigma(T)$ for mafic rocks is very significant at $T < 500$ ° C (Fuji-ta et al., 2004). The extrapolated $\sigma \approx 10^{-7}$ S/m is much lower than that of a peridotite below the Moho, assessed from the field conductivity measurements, ≈10^{-2} S/m by Jones (1999), but close to the experimentally measured values in dry olivine, from ≈ 3 × 10^{-8} to 10^{-9} S/m at T≈ 450–465 °C, by Xu et al. (2000). In the astenosphere, at $d > 210$ km, the electrical condustivity is $10^{-3} < \sigma < 10^{-2}$ S/m, which is typical for σ in the sub-lithospheric upper mantle (Bahr and Duba, 2000). The lithosphere–astenosphere transition in the model is marked by a significant drop in σ (Fig. 3)

at depth ≈200–210 km. The high-T garnet peridotites that represent the astenosphere and have been metasomatized by astenospheric melts, possess much higher ϱ than the overlaying fertile peridotite. The chemical composition of rocks at the depth ≈200 km changes significantly. According to (Kopylova and Russel, 2000), on the boundary between fertile peridotite and high-T gar peridotite the olivine content in rocks increases from about 60 to 77 vol.%, Cpx decreases from 11 to 2.6%, and garnet decreases from 12.5 to 5.1%. This is also accompanied by the increase of Mg-number from 0.88 to 0.91 and increase of Mg/Si ratio from 1.08 to 1.32. Below 240 km, the variation of $\sigma(d)$ with d is much smaller while $T(d)$ follows the adiabatic gradient: $(\mathrm{d}T/\mathrm{d}z)_S = gT\alpha/C_p \sim 0.25 \div 0.3$ km, where $g = 9.81\ \mathrm{m^2/s}$, $T = 1673$ K, $\alpha = 2 \times 10^{-5}\ \mathrm{K^{-1}}$, $C_p = 1240\ \mathrm{J\,kg^{-1}\,K^{-1}}$.

4. Modelled MT-response

For the modelled $\sigma(d)$ (Fig. 3), the apparent resistivity (ϱ_a) and the phase shift (Φ) between electric and magnetic field vectors of a potential magnetotelluric response (MT) have been calculated for the 1D magnetotelluric forward modeling with the help of a Wait-algorithm (Wait, 1972). The MT-response of the model is shown in Fig. 4. The calculated MT-response differs from the average MT-response obtained from all sations in the Slave craton region (Jones et al., 2003). The data from the station Lac de Gras indicate a slightly lower electrical resistance than the model. At periods < 1 s, ϱ_a, for the suggested $\sigma(d)$, agrees with the average field data. At periods > 1 s ϱ_a of the model is lower than that of the average MT-inversion but is still higher than the resistance obtained from the Lac de Gras station (Jones et al., 2003). For Φ, the agreement between the MT-data with the model is not good starting from the periods > 0.1 s, but there is a satisfactory agreement at periods $> 10^3$ s for the Lac de Gras station of Central Slave.

The disagreement between modelled and observed MT-responses may be due to several factors: (a) The presence of conductive granulites in the lower crust may decrease the quality of the model inversion in the mantle below the Moho due to a shielding effect. On the other hand, the data of Jones and Ferguson (2001) indicate a very unusual nonconducting lower crust beneath the Slave craton. (b) In the $\sigma(d)$ model, the temperature dependence of $\sigma(T)$ obtained in laboratory has been extrapolated to very high and low temperatures. This extrapolation, especially at low temperatures, may result in an overestimation of the electrical conductivity on the Moho boundary. (c) The chosen averaging procedure to

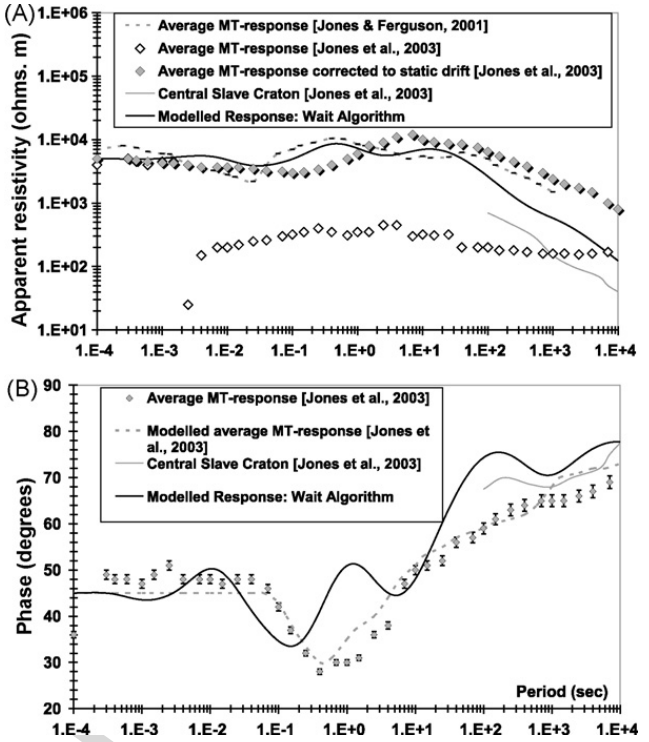

Fig. 4. Modeled MT-response of $\sigma(d)$ from Fig. 3 obtained with the Wait-algorithm (Wait, 1972). (A) The apparent resistivity ϱ_a, Ω m (error bars are about the size of symbols), (B) the phase shift Φ, °. Average MT-responses obtained from the inversion of the MT-data of all station (Jones and Ferguson, 2001) and the MT-response from Central Slave, the station Lac de Gras (Jones et al., 2003) are shown for comparison.

calculate $\sigma(T)$ from a rock mixture is oversimplified. The changes of mineralogy of rocks and in temperature are also accopanied by a continiuos variation of the redox state of Fe^+ which is difficult to take into account in mixing models of electrical conductivity. (d) The numerical modelling of the MT-response is based on the simplistic geometry and boundary conditions, 2D effects of rock layering were not included in the direct modelling procedure.

5. Conclusions

The difference between the average Slave MT inversion and $\sigma(d)$ from the laboratory measurements in Fig. 3 indicates that the mineralogy and electrical properties of peridotites in general can be accounted for in the observed electrical conductivity in the Central Slave craton mantle. Our data can to some extent explain the nature of a conductive layer beneath Central Slave craton by the presence of fertile peridotites overlaying much less conductive layers of high-T garnet peridotites. The contrast between σ of these two rocks is about one order of magnitude (see Fig. 2).

(1) The Central Slave mantle conductor mapped at depths with the dominated depleted spinel peridotite mineralogy cannot be explained fully with the increased σ due to the depleted spinel peridotite. As follows from $\sigma(T)$ measurements (Fig. 2), the spinel peridotites have similar σ as garnet peridotites.

(2) The mineralogy of the resistive high-T astenospheric peridotite cannot be responsible for the conductive asthenosphere. The changes in the mineralogy between the low-T lithospheric peridotite and high-T asthenospheric peridotite fail to be accounted for in the enhanced σ in the astenosphere beneath the Central Slave craton. However, it is possible that a smaller grain size in the Slave high-T peridotites, most of which are sheared (Kopylova et al., 1999; Menzies et al., 2004), makes the astenosphere more conductive according to experiments with sintered olivine powder compacts (ten Grotenhuis et al., 2004). The presence of eclogites in the Slave mantle are unlikely to contribute to the observed discrepancy between the modelled and the observed MT-responses. Eclogite rocks in general possess smaller activation energy of σ than peridotites, $E_a \sim 0.7$ eV (Lastovickova, 1975) in comparison with olivine-rich rocks, which makes the overall depth increase of σ less steeper in comparison with eclogite-free upper mantle rocks.

References

Artemieva, I., Mooney, W., 2001. Thermal thickness and evolution of Precambrian lithosphere: a global study. J. Geophys. Res. 106, 16387–16414.

Artemieva, I., Mooney, W., 2002. On the relations between cratonic lithosphere thickness, plate motions, and basal drag. Tectonophysics 358, 211–231.

Bahr, K., Duba, A., 2000. Is the astenosphere electrically anisotropic? Earth Planet Sci. Lett. 178, 87–95.

Bank, C.-G., Bostock, M.G., Ellis, R.M., Cassidy, J.F., 2000. A reconnaissance teleseismic study of the upper mantle and transition zone beneath the Archean Slave craton in NW Canada. Tectonophysics 319, 151–166.

Bleeker, W., 2003. The late Archean record: a puzzle in ca. 35 pieces. Lithos 71, 99–134.

Boerner, D.E., Kurtz, R.D., Craven, J.A., Ross, G.M., Jones, F.W., Davis, W.J., 1999. Electrical conductivity in the Precambrian lithosphere of Western Canada. Science 283, 668–670.

Brey, G.P., Köhler, T., 1990. Geothermobarometry in four-phase lherzolite. II. New thermobarometers, and practical assessment of existing thermobarometers. J. Petrol. 31, 1352–1378.

Constable, S., 1993. Constraints on mantle electrical conductivity from field and laboratory measurements. J. Geomagn. Geoelectr. 45, 707–728.

Constable, S., 2006. SEO3: a new model of olivine electrical conductivity. Geophys. J. Int. 166, 435–437.

Constable, S., Shankland, T.J., Duba, A., 1992. The electrical conductivity of an isotropic olivine mantle. J. Geophys. Res. 97, 3397–3404.

Davis, W.J., Jones, A.G., Bleeker, W., Grütte, H., 2003. Electric lithosphere of the Slave craton. Lithos 71, 575–589.

Fuji-ta, K., Katsura, T., Tainosho, Y., 2004. Electrical conductivity measurements of granulite under mid- and lower crustal pressure–temperature conditions. Geophys. J. Int. 157, 79–86.

Griffin, W.L., O'Reilly, S.Y., 1987. The composition of the lower crust and the nature of the continental Moho, xenolith evidence. In: Nixon, P.H. (Ed.), Mantle Xenoliths. John Wiley, NY, pp. 413–430.

Griffin, W.L., Doyle, B.J., Ryan, C.G., Pearson, N.J., O'Reilly, S.Y., Davies, R., Kivi, K., van Achterbergh, E., Natapov, L.M., 1999. Layered mantle lithosphere in the Lac de Gras Area, Slave craton: composition, structure and origin. J. Petrol. 40 (5), 705–727.

Ingham, M.R., 1997. Electrical resistivity structure of the Canterbury Plains, New Zealand. NZ J. Geol. Geophys. 40 (4), 465–471.

Jones, A.G., 1999. Imaging the continental upper mantle using electromagnetic methods. Lithos 48, 57–80.

Jones, A.G., Ferguson, I.J., 2001. The electric Moho. Nature 409, 331–333.

Jones, A.G., Ferguson, I.J., Chave, A.D., Evans, R.L., McNeice, G.W., 2001. Electrifying images of the Slave craton. Geology 29 (5), 423–426.

Jones, A.G., Lezaeta, P., Ferguson, I.J., Chave, A.D., Evans, R.L., Garcia, X., Spratt, J., 2003. The electrical structure of the Slave craton. Lithos 71, 505–527.

Kopylova, M.G., Garo, G., 2004. Mantle xenoliths from South-eastern Slave Craton: evidence for chemical zonation in a thick, cold lithosphere. J. Petrol. 45 (5), 1045–1067.

Kopylova, M.G., Russel, J.K., 2000. Chemical stratification of cratonic lithosphere: constraints from Northern Slave craton, Canada. Earth Planet Sci. Lett. 181, 71–87.

Kopylova, M.G., Russell, J.K., Cookenboo, H., 1999. Petrology of peridotite and pyroxenite xenoliths from the Jericho Kimberlite: implications for the thermal state of the mantle beneath the Slave Craton, Northern Canada. J. Petrol. 40 (1), 79–104.

Lastovickova, M., 1975. The electrical conductivity of eglogites measured by two methods. Stud. Geoph. Geod. 19 (4), 394–398.

Ledo, J., Jones, A.G., 2005. Upper mantle temperature determined from composition, electrical conductivity laboratory studies and magnetotelluric field observations: Application to the intermontane belr, Northern Canadian Cordillera. Earth Planet Sci. Lett. 236, 258–268.

Lichtenecker, K., 1926. Die Dielektrizitätskonstante natürlicher und künstlicher Mischörper. Phys. Zeitschr 27, 115.

McCammon, C., Kopylova, M.G., 2004. A redox profile of the Slave mantle and oxygen fugacity control in the cratonic mantle. Contrib. Miner. Petrol. 148, 55–68.

Maumus, J., Bagdassarov, N.S., Schmeling, H., 2005. Electrical conductivity and partial melting of mafic rocks under pressure. Geochim. Cosmochim. Acta 69 (19), 4703–4718.

Menzies, A., Westerlund, K., Gurney, J., Carlson, J., Fung, A., Nowicki, T., 2004. Peridotitic mantle xenoliths from kimberlites on the Ekati Diamond Mine Property, NWT, Canada: major element compositions and implications for the lithosphere beneath the Central Slave craton. Lithos 77, 395–412.

Parkhomenko, E.I., 1967. Electrical Properties of Rocks. Plenum Press, NY, p. 314.

Pearson, N.J., Griffin, W.L., Doyle, B.J., O'Reilly, S.Y., van Achterbergh, E., Kivi, K., 1999. Xenoliths from kimberlite pipes of the Lac de Gras area, Slave Craton, Canada. In: Gurney, J.J., Gurney, J.L.,

Pascoe, M.D., Richardson, S.H. (Eds.), Proceedings of the Seventh International Kimberlite Conference on Red Roof Designs, vol. 2, The P.H. Nixon, Cape Town, pp. 644–658.

Russel, J.K., Dipple, G.M., Kopylova, M.G., 2001. Heat production and heat flow in the mantle lithosphere, Slave craton, Canada. Phys. Earth Planet Inter. 123, 27–44.

Sakamoto, D., Yoshiasa, A., Yamanaka, T., Ohtaka, O., Ota, K., 2002. Electric conductivity of olivine under pressure investigated using impedance spectroscopy. J. Phys.: Condens. Matter. 14, 11375–11379.

Schultz, A., Kurtz, R.D., Chave, A.D., Jones, A.G., 1993. Conductivity discontinuities in the upper mantle beneath a stable craton. Geophys. Res. Lett. 20 (24), 2941–2944.

Sleep, N.H., 2003. Survival of Archean cratonal lithosphere. J. Geophys. Res. 108, 2302.

Sleep, N.H., 2005. Evolution of the continental lithosphere. Annu. Rev. Earth Planet Sci. 33, 369–393.

ten Grotenhuis, S.M., Drury, M.R., Peach, C.J., Spiers, C.J., 2004. Electrical properties of fine-grained olivine: Evidence for grain boundary transport. J. Geophys. Res. 109, B06203.

Tyburczy, J.A., Fisler, D.K., 1995. Electrical properties of minerals and melts. In: Ahrens, J. (Ed.), A Handbook of Physical Constants, II. Mineral Physics and Crystallography. AGU, Washington, DC, pp. 185–208.

Wait, J.R., 1972. Electromagnetic Waves in Stratified Media. Pergamon Press, NY, p. 314.

Xu, Y., Shankland, T.J., Duba, A.G., 2000. Pressure effect on electrical conductivity of mantle olivine. Phys. Earth Planet Inter. 118, 149–161.